

Microparticle-assisted 2D super resolution virtual image modeling

Bekirov A.R., Zengbo W., Luk'yanchuk B.S.

ABSTRACT

The approach that makes it possible to explain the phenomenon of super resolution in a virtual image using dielectric microparticles is presented. A resolution of 100 nm in the visible range is demonstrated, resolutions of the order of 50 nm are being discussed. The presented two-dimensional model uses the FDTD code to analyze the generation of radiation and propagation through a system of slits in a metal screen and a dielectric microparticle located above it. The image is constructed using the back propagation method.

INTRODUCTION

The wave nature of light limits the size of objects that can be observed using an optical microscope. According to the Abbe criterion, it is impossible to distinguish two point incoherent sources if the distance between them is less than half the wavelength $\lambda/2$ of the emitted radiation. In [1] it was shown that by examining objects with the help of dielectric particles, it is possible to resolve structures beyond the diffraction limit, i.e. whose size is significantly less than half the wavelength. Various theories have been proposed to explain this phenomenon [2-7]. However, no clear explanation of the nature of this phenomenon has been presented. In order to explain the theoretical problems that arise, it is necessary to consider in more detail the process of image formation by a microparticle. It is convenient to carry out this consideration using geometric optics.

While observing an object through a microsphere, for example, a point source, the ray path is changed due to refraction at the microparticle boundary, Fig. 1. As a result, a magnified virtual image is formed. The observed distance between the two sources also increases, however, it would be a mistake to say that such consideration can explain the overcoming of the diffraction limit. The rays forming the virtual image are concentrated inside a cone whose boundaries touch the surface of the sphere (Fig. 1). As a result, the numerical aperture that forms the image is limited, and blurring of the image occurs, which compensates for the gain due to magnification. In addition, because of aberration not all refracted rays converge at one point.

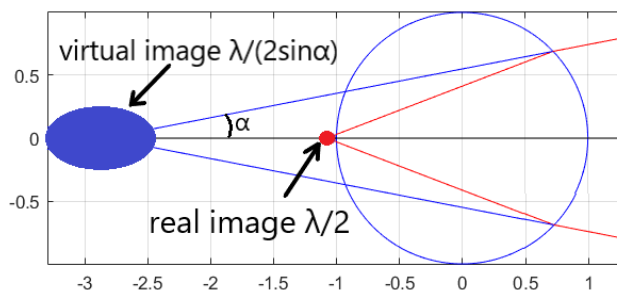


Fig. 1. Geometric path of rays from a point source. Red rays are the actual path of the rays, blue ones form a virtual image and are a continuation of the red ones during reverse propagation. The blue and red dots show the size for the real and virtual images. The image in the virtual case is significantly blurred due to the limited viewing angle.

This consideration was carried out from the standpoint of geometric optics, which has a limited area; in our example, the condition of applicability is the smallness of the light wavelength compared to the particle size. In experiments, the particle size ranges from several to tens of

wavelengths [1, 8]. Thus, it is advisable to consider this problem from the standpoint of wave optics. However, the wave theory in the most of cases demonstrates agreement with geometric considerations [5]. The exception is serious cases. In [4], it was firstly demonstrated that when exciting the whispering gallery modes with a dipole, it is possible to increase the resolution to $\lambda/4$. However, as emphasized in the work, this requires a very special choice of the wavelength or radius of the sphere. Typically, in experiments, super-resolution is observed using a broadband light source in microparticles of various sizes. Thus, a correct theory should not rely on resonance phenomena of this type. In addition, the distributions presented in [4] for the image field have significant “noise” around the focusing point, which is also not observed in the experiment.

The situation changes significantly when the substrate is taken into account. In this case, there are rays arising due to re-reflection of the “sphere-substrate” type. In work [9], we showed that in a particle-on-substrate system it is possible to form magnification without blurring. The resolution of $\lambda/8$ was showed. However, some modification in the solution is required. In the first case, a change in the source field, in the second, a change in the scattering matrix of the sphere. In both cases, the required amendments made a huge contribution to the original solution. It is important to note that such the amendments are the only ones! Thus, despite the fact that the work was of a very formal nature, it showed that the required properties of the system to overcome the diffraction limit differ very significantly from those considered before. It suggests that it is necessary to consider more complex effects of the type of interaction between the microparticle and the object. To this end, we propose to consider a complete simulation of the propagation of radiation from an object through a microparticle and subsequent image formation. Due to the large requirements for computing power, we will limit ourselves to the two-dimensional case.

RESULTS

To present our model we start from simulation of the results from work [1]. The experiment used an incoherent source in the form of a halogen lamp. The first step requires constructing a source field. We used data on the spectrum of this source from work [2], see Fig. 2, since in the original work only the peak wavelength was indicated. Note that further results do not change if we consider a uniform spectrum from 425 nm to 675 nm. To simulate source field we used point sources with random frequency and initial phase. The wavelengths are distributed with probability according to the spectrum in Fig. 2. The initial phases had a uniform distribution from 0 to 2π .

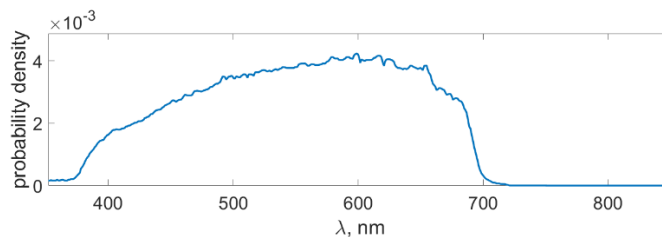


Fig. 2. Probability density distribution for source frequencies used in our the calculations according [2].

In our simulation we used 2D FDTD method in the TE geometry ($E_z=0$) implemented in the Lumerical MODE package. Note that we used a custom time signal in the form of a continuous emission, rather than a single pulse. To construct the image, we used the idea of backpropagation of radiation. For this purpose, the same 2D FDTD method implemented in the custom Matlab code was used. In order to generate an image, the radiation sources must be real fields, but taken in reverse time. In our example, the source was a single component H_z

$$H_z^{image\ source}(t) = H_z^{real\ field}(-t). \quad (1)$$

To record the real field, we used time-monitors located above the sphere. Note that the resulting image field does not depend on the location of time-monitors. To present time-independent result we use time averaging of the image field intensity:

$$I^{image}(x, y) = 1/T \int_0^T |\mathbf{E}^{image}(x, y, t)|^2 dt, \quad (2)$$

here T - is the total simulation time.

Firstly, we simulate super resolution for slits in metal screen. In this case, the sample was observed in the transmitted light mode. The sample is a 30 nm thick perfect conductive screen coated on the glass substrate with four 360 nm wide slits at the distance of 130 nm . The glass microparticle (SiO_2) with a radius of $2.37 \mu\text{m}$ is located above the slits according to Figure 3. We simulated four slits offset from the center of the sphere to ensure that the maxima in the image field actually reflect the location and number of slits. The sources were located in the glass substrate $3 \mu\text{m}$ below the slits. The simulation time was 1000 fs , repeated 100 times and averaged over all implementations. The simulation results present in Fig. 3. According to the results presented in Figure 3, the microparticle makes it possible to distinguish slits, while in free space they are indistinguishable. We plotted the square of the average intensity $(I^{image})^2$, which does not affect on the resolution but gives better contrast. The three maxima in Fig. 3.b arise due to the limited averaging time.

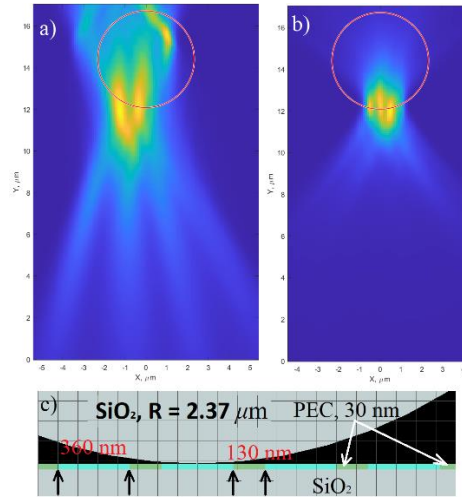


Fig. 3. a, b) – time-averaged image field with and without a microparticle, respectively. Comparing distributions a) and b) we can conclude that the gaps are indistinguishable without the presence of a microparticle. For better contrast we used square of the values (2) c) general calculation scheme, four 360 nm slits with a step of 130 nm between them in a 30 nm thick perfect conductive screen. The entire system is located on a glass substrate, inside of which there are sources with a random phase and frequency. A glass sphere with a radius of $2.37 \mu\text{m}$ is located above the slits.

Next, we consider Blue ray DVD disk super resolution in the reflection mode. For simulation in reflection mode, sources should be placed above the microparticle. In order to exclude the field of sources when the field is reversed in time, we used directed Gaussian sources. In this case, the source field extends only towards the object. We presented the DVD disc as perfect conductors embedded in SiO_2 with dimensions corresponding to the DVD disc, 20 nm thickness perfect conductors 200 nm wide at 100 nm distance, see Fig 4. In order to show that resonance effects do not play a role in this case we took the radius of the particle $R = 2.35 \mu\text{m}$. The simulation result present in Fig. 4.

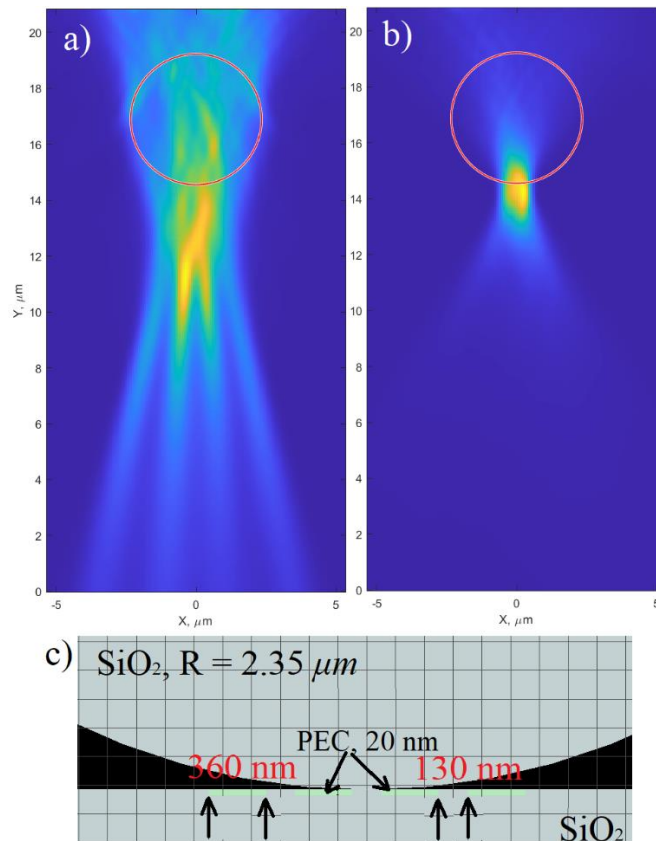


Fig. 4. a, b) – time-averaged image field in reflection mode with and without the microparticle, respectively. Comparing distributions a) and b) we can conclude that the gaps are indistinguishable without the presence of a microparticle. For better contrast we used square of the values (2) c) general calculation scheme, four perfect conductors 200 nm wide at 100 nm distance.

Next we will look at image simulation for 50 nm pores in gold-coated anodic aluminium oxide (AAO) membrane. Modeling a sample over its entire thickness is a very cumbersome task, so we limited the aluminum layer to 2 μm, the gold layer is 30 nm. The entire sample is divided into 50 nm pores with 50 nm distances between them. The microparticle size is similar to the previous calculation, $R = 3 \mu\text{m}$. The radiation sources were 200 point dipoles at a distance of 1.2 μm from the lower boundary of aluminum. The simulation results are presented in Fig. 5.

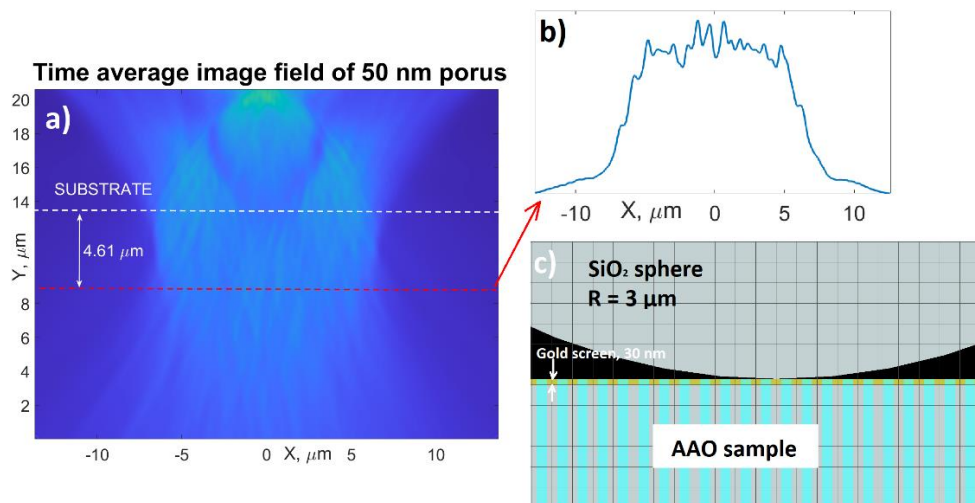


Fig. 5. a) time-averaged image field, the white line indicates the position of the screen, the red line indicates the slice in which three pronounced maxima can be observed. b) image field at a distance of 4.61 μm below the screen. c) sample diagram, 50 nm pores with a distance of 50 nm between them in a 2 μm thick aluminum substrate and 30 nm gold.

At a distance of $4.61 \mu\text{m}$ below the substrate, three pronounced maxima can be observed. However, it would be a mistake to assume that the resolution is 50 nm . Because the three distinct pores remain indistinguishable. Thus, from our simulations, we can conclude that the presented experiment is not reliable evidence of super resolution of 50 nm , since we see only some maxima but cannot claim that these maxima correspond to several adjacent pores.

For a more reliable check, you should consider individual objects rather than periodic ones. For this purpose, we considered a similar calculation, but for only two objects. Unfortunately, the approach we presented does not provide convincing evidence of the distinguishability of pores at a distance of 50 nm with halogen field source. However, there are works in which individual objects were observed at distances of the order of 50 nm [11, 12]. In those works the imaging was performed by a scanning laser confocal microscope operating at $\lambda = 405 \text{ nm}$. According to that scheme we simulate super resolution for two perfect conductive 120 nm wide dimers at 60 nm distance according to work [11] and 136 nm wide dimers at 26 nm distance according to [12]. We used a reflection mod, similar to what we did for the DVD disc above. All sources had the same wavelength $\lambda = 405 \text{ nm}$, but random phase. We used the same material SiO_2 for microparticle. The obtained results presented in Fig. 6. Both cases demonstrate super resolution for fixed wavelength $\lambda = 405 \text{ nm}$ of source as it was observed in experiment. We also carried out the calculation in the absence of microparticles. In both cases the picture does not change, the structures are not distinguishable, see Fig. 6 c).

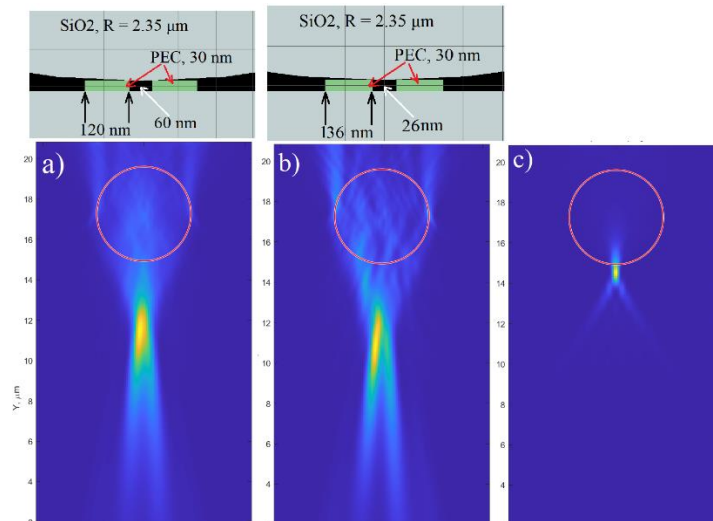


Fig. 6. Virtual image for dimers in the reflection mode with $\lambda = 405 \text{ nm}$ for a) 120 nm wide dimers at 60 nm distance, b) 136 nm wide dimers at 26 nm distance. The calculation geometry is shown in the top panels. c) image when there is no particle, the same for both cases.

Our calculation states that the source field and its spectrum is a crucial parameter for microparticles assisted super resolution technique. The optical resolution criterion $\lambda/2$ accepted in the literature refers to two point sources. The question of the applicability of this criterion to real objects is widely discussed [12], in particular whether the distance between the edges of structures should be compared or with their centers. In all the presented results, the spectrum of the source contains wavelengths comparable to the size of the structures, which allows us to conclude that the sphere increases contrast, not resolution. However, our model is still not complete, 2D simulation not allow to simulate more complex shapes, as a triangle or star. In addition, we used ideal conductors to model the structures, which significantly reduced the overall modeling time. However, the results we presented can serve as a reliable foundation for further 3D modeling.

CONCLUSIONS

This paper presents a calculation that makes it possible to explain most of the phenomena observed in [1, 11, 12]. Our results provide convincing evidence of the distinguishability of structures with dimensions similar to Blue-ray DVD discs. We have shown that when considering AAO structure with a period of about 50 nm, pronounced maxima can be observed in the virtual image, but we cannot attribute their presence to super-resolution at these scales, since we cannot distinguish individual objects at such a distance for halogen lamp source. We showed super resolution of the order of 50 nm at a wavelength of $\lambda = 405$ nm as it was in [11-12]. Our calculations show that microparticle assisted microscopy allows to distinguish objects comparable with wavelength of light even the distance between them much less. However, when using the FDTD method, we could have missed resonance solutions. In order to verify the correctness of our approach, it is necessary to conduct a full 3D modeling.

BIBLIOGRAPHY

- [1] Wang, Zengbo, et al. "Optical virtual imaging at 50 nm lateral resolution with a white-light nanoscope." *Nature communications* 2.1 (2011): 218.
- [2] Yang, Hui, et al. "Super-resolution imaging of a dielectric microsphere is governed by the waist of its photonic nanojet." *Nano letters* 16.8 (2016): 4862-4870.
- [3] Boudoukha, Rayenne, et al. "Near-to far-field coupling of evanescent waves by glass microspheres." *Photonics*. Vol. 8. No. 3. MDPI, 2021.
- [4] Duan, Yubo, George Barbastathis, and Baile Zhang. "Classical imaging theory of a microlens with super-resolution." *Optics letters* 38.16 (2013): 2988-2990.
- [5] Bekirov, Arlen Remzievich, B. S. Luk'yanchuk, and Andrei Anatol'evich Fedyanin. "Virtual image within a transparent dielectric sphere." *JETP Letters* 112.6 (2020): 341-345.
- [6] Pahl, Tobias, et al. "FEM-based modeling of microsphere-enhanced interferometry." *Light: Advanced Manufacturing* 3.4 (2022): 699-711.
- [7] Simovski, Constantin, and Reza Heydarian. "A simple glass microsphere may put the end to the metamaterial superlens story." *AIP Conference Proceedings*. Vol. 2300. No. 1. AIP Publishing, 2020.
- [8] Lee, Seungjun, et al. "Overcoming the diffraction limit induced by microsphere optical nanoscopy." *Journal of Optics* 15.12 (2013): 125710.
- [9] Bekirov, A. R. "On superresolution in virtual image in a transparent dielectric sphere." *Optics and Spectroscopy* 131.3 (2023).
- [10] Bekirov, Arlen R., et al. "Wave theory of virtual image." *Optical Materials Express* 11.11 (2021): 3646-3655.
- [11] Yan, Y., Li, L., Feng, C., Guo, W., Lee, S., & Hong, M. (2014). Microsphere-coupled scanning laser confocal nanoscope for sub-diffraction-limited imaging at 25 nm lateral resolution in the visible spectrum. *Acs Nano*, 8(2), 1809-1816.

[12] Allen, Kenneth W., et al. "Super-resolution microscopy by movable thin-films with embedded microspheres: resolution analysis." *Annalen der Physik* 527.7-8 (2015): 513-522.